ZTEM Airborne Natural Field EM-Magnetics and Mineral Targeting Results over the Berg Porphyry Copper Project, near Houston, British Columbia.

Jean M. Legault
Geotech Ltd.
Aurora ON CAN
Jean.legault@geotechairborne.com

Karl Kwan
Geotech Ltd.
Aurora ON CAN
karl.kwan@geotechairborne.com

Shane Ebert
Surge Copper Corp.
Vancouver BC CAN
shane@surgecopper.com

SUMMARY

A ZTEM natural field helicopter EM and magnetic survey was flown over the Berg copper-molybdenum-silver project in the Huckleberry district, near Houston in central British Columbia, Canada. Mineralisation at Berg surrounds a quartz monzonite intrusion. Analyses of the airborne geophysical responses, using 2D-3D inversions, show combined well-defined ring-like resistivity low surrounding a resistive core and similar annular magnetic high and low signatures over the known and suspected porphyry deposits, similar to those previously found in ZTEM surveys over other porphyry deposits in the Western Cordillera. A mineral targeting approach is implemented that uses a semi-automated, machine-learning (ML) assisted method that includes: Structural Complexities (SC), Self-Organizing Map (SOM) classifications, and Supervised Deep Neural Network (SDNN) targeting of the geophysical data. The new targeting approach has identified both the Berg and Bergette porphyry copper occurrences, as well as two others our areas for follow-up that also host known mineral showings.

Key words: Porphyry copper, ZTEM, electromagnetics, resistivity, magnetics, 3D inversion, mineral targeting.

INTRODUCTION

In May 2021, Surge Copper Corp. announced plans for a new district wide exploration program over its Ootsa and Berg Projects in the Huckleberry district, near Houston, north central British Columbia, including a ZTEM (Z-axis Tipper Electromagnetic; Lo and Zang, 2008) geophysical survey (Surge, 2021). The Ootsa-Berg project (Figure 1) is host to 4 advanced porphyry projects, including the undeveloped Berg copper-molybdenum-silver porphyry deposit. In June-July 2021 a ZTEM helicopter natural field electromagnetic and magnetic survey was flown over Ootsa-Berg and the results that focus on the Berg porphyry copper deposit and nearby occurrences are described in this study.

The Berg and Ootsa properties are adjoined on the west side, with Berg project lying immediately northwest of Imperial Metals' Huckleberry porphyry Cu-Mo-Ag mine and mill complex, and the Ootsa property to the southeast (Figure 1). The two properties cover a total combined area of >120,000 hectares and encompass the Seel-Huckleberry-Berg porphyry trend. The Berg claims were initially prospected in the late 1920's by Cominco but the Berg porphyry system was discovered by Kennecott following trenching and drilling in 1964. Subsequent exploration drilling by operators Placer Dome, Terrane Metals, Thompson Creek Metals, Centerra Gold and now Surge Copper total over 56,000 m in 224 holes. A resource estimate in 2021 established a measured and indicated mineral resource of 610 Mt grading 0.27% Cu, 0.03% Mo and 3 g/t Ag. The Berg deposit currently remains undeveloped (Norton et al., 2021).

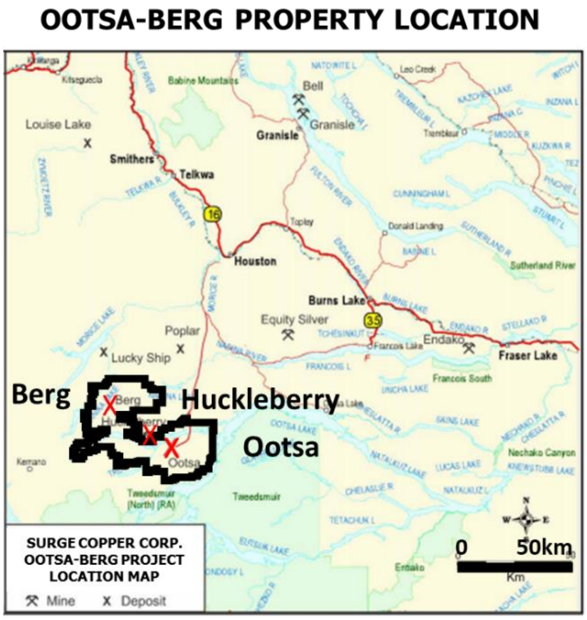

Figure 1: Ootsa-Berg Property location, showing nearby Huckleberry Mine and regional deposits in north central British Columbia (modified after Purich et al., 2016).

ZTEM (z-axis tipper electromagnetic; Lo and Zang, 2008; Legault et al., 2012) helicopter natural field EM has been widely used in porphyry copper exploration for >15 years in mapping resistivity contrasts that characterize porphyry copper deposit alteration systems (Hoschke, 2011). ZTEM case-study examples over porphyry deposits include Lo and Zang (2008) in Safford, Arizona; Holtham and Oldenburg, (2010) at Bingham Canyon, Utah, Izarra et al. (2011) at Copaquire, Chile, and Burge (2014) at Cobre Panama. ZTEM examples in Western Cordillera include Sattel et al. (2010) at Mt Milligan, BC, and Lee et al. (2017) at Morrison, BC, and Paré et al. (2012) at Pebble, Alaska.

The Berg ZTEM-Magnetic case study has been presented in Legault et al. (2022). This paper adds to that study by presenting a new targeting approach, described in Legault (2023ab) that uses a semi-automated, machine-learning (ML) assisted approach that includes: Structural Complexities (SC), Self-Organizing Map (SOM) classifications, and Supervised Deep Neural Network (SDNN) approach to mineral targeting.

Geology and Mineralisation

Berg (Figure 2) is a classic calc-alkaline Cu-Mo porphyry deposit, which are typically marked by complex alteration zones that are usually centred around an intrusive complex. The Berg mineralisation forms an annulus along the contact between the 50 Ma quartz monzonite stock and the hornfelsed Hazelton Group volcanic rocks and quartz diorite which it intrudes (Norton et al., 2021).

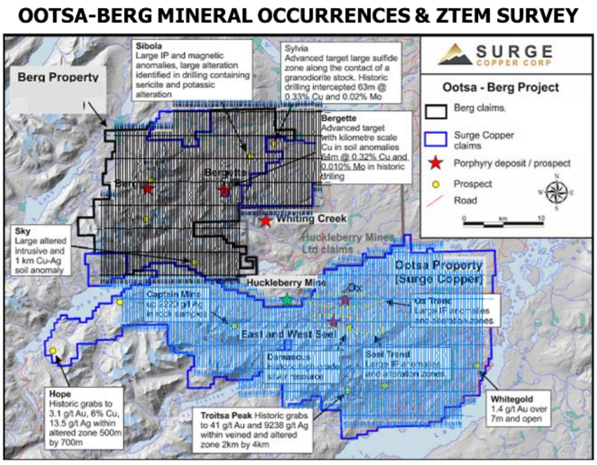

Figure 2: Plan view of the Ootsa-Berg porphyry project, showing the four main porphyry occurrences (Berg, Bergette, Ox, Seel) and nearby Whiting Creek prospect and Huckleberry Mine (green star), with ZTEM flight lines (Berg-black & Ootsa-blue) overlaid on contoured topography (modified after www.surgecopper.com).

Hypogene mineralisation at Berg is characterised by several generations of veining. Disseminated mineralisation containing copper and molybdenum is only important in the outer anulus of the quartz monzonite stock and in the adjacent volcanic rocks and quartz diorite. Associated alteration envelopes are either potassic or sericitic. A well-developed supergene enrichment blanket is superimposed on the hypogene mineralisation, and consists mainly of chalcocite, covellite and digenite, with trace amounts of copper oxides in the overlying leached cap. The surrounding phyllic and propylic alteration zones are typically poor in Cu+/-Mo sulphides (Norton et al, 2021). Mineralisation at Berg is open to depth and outward from the Berg monzonite Stock. The deposit has been shown to have excellent vertical continuity with significant mineralisation intersected greater than 550m below surface (www.surgecopper.com).

Another known mineral occurrence of importance on the Berg property is the Bergette prospect that lies 10 km east of the Berg deposit (Figure 2-Figure 3). Bergette consists of a large gossan and mineralisation is marked by strong Cu-Mo response in soils, across a 2x5 km northeast trending zone. Limited drilling and mapping indicate that Bergette is underlain by Hazelton Group volcanic and sedimentary rocks, intruded by granodioritic Sibola stock. Sulphides occur in breccias and fractures. An AeroTEM III (Allard, 2007) helicopter TDEM survey over the Berg-Bergette area in 2010 shows that Bergette has a similar size resistivity response (Norton et al., 2021).

At the Tara/Sibola occurrence, roughly 5.5 km NE of Bergette (Figure 2 & Figure 3), low-grade porphyry-style mineralisation is hosted in a felsic stock and occurs within the central part of a broad qtz-sericite-pyrite alteration zone (S. Ebert, SCC, pers. comm., 03-2022).

METHOD AND RESULTS

Helicopter ZTEM Natural Field EM and Magnetic Survey

Helicopter-borne geophysical surveys were carried out over the Ootsa-Berg Project from June 8th to 30th, 2021, on behalf of Surge Copper Corp. Principal geophysical sensors included a Z-Axis Tipper electromagnetic (ZTEM) system (Lo and Zang, 2008), and a caesium magnetometer. Two Geotech ZTEM base station sensors measured the orthogonal, horizontal X and Y components of the natural EM field. Data from the three coils are used to obtain the Tzx and Tzy Tipper (Labson et al., 1985) in-phase and quadrature components at six frequencies in the 30 to 720 Hz band. A total of 4,224 line-kilometres were flown, including approximately 1,779 line-km at Berg, along 300m spaced, north-south oriented flight lines and 3 km spaced east-west tie lines. The nominal EM bird terrain clearance was 85 metres, and magnetic sensor clearance was 100 metres. The Berg survey block is relatively rugged, with >1,600 m of vertical relief, particularly in the Berg porphyry region (Figure 2).

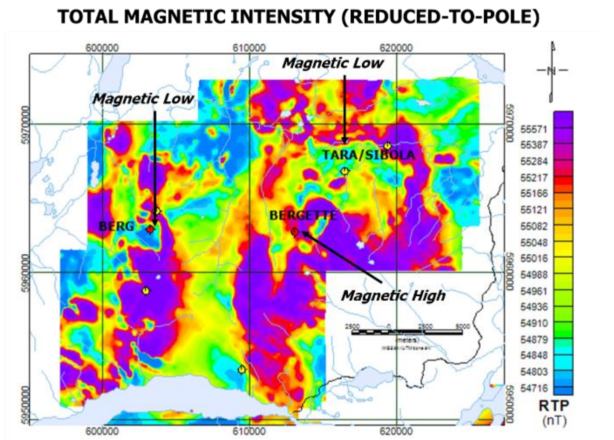

Figure 3: Total magnetic intensity (reduced to pole), showing Berg porphyry and other occurrences from Figure 2, and highlighting some features of interest.

ZTEM and Magnetic Survey Results

Figure 3 presents the reduced to pole (RTP) total magnetic intensity results, and the corresponding Berg porphyry and other mineral occurrences from Figure 2. The magnetic results highlight a prominent, large (~1.5x1.5 km), magnetic low feature centred on the Berg porphyry, which is in turn surrounded by a reverse C-shaped magnetic high. Worthwhile noting that similar ring-like magnetic patterns observed over the porphyry copper cluster at Cobre Panama are interpreted to represent demagnetized areas due to porphyry-related phyllic alteration (Burge, 2014; Legault et al., 2016). Conversely, Bergette lies within a magnetic high but is indistinct. Tara/Sibola occurs in low magnetic rocks but lies adjacent to a small, intrusion like magnetic high feature. Other distinctive circular or ring-like magnetic high and low signatures are noted across the Berg Project.

The RTP magnetic data were then analysed for structural complexity (SC), using the Geosoft CET (Center for Exploration Targeting) grid analysis tool (Holden et al., 2012). The CET SC analysis tool outputs two parameters: i) the Contact Orientation Density (COD), and the Orientation Entropy (OE). Figure 4 presents the SC-derived COD image. As shown, the structural complexity highs are concentrated in areas with porphyry occurrences.

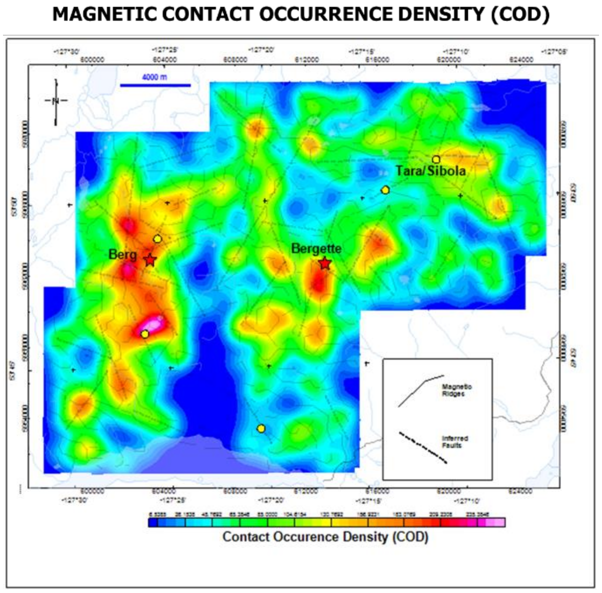

Figure 4: Structural complexity (SC) analysis of magnetic data, showing the Contact Occurrence Density (COD), over mineral occurrences and inferred faults (dashed lines), and magnetic ridges.

Figures 5ab present the ZTEM tipper data, displayed as both Total Phase Rotation and Total Divergence (DT; Lo and Zang, 2008) at the 90 Hz frequency. The TPR and DT image map resistivity variations in plan, in addition to artefacts caused by topography (Sattel and Witherly, 2012). The TPR and DT image highlights the pronounced circular or ring-like pattern anomaly over the Berg porphyry, which also agrees with the annular geology and alteration patterns that occur within the deposit. Similar ring-like patterns are observed in ZTEM data over other porphyries in Western Cordillera, such as Pebble, Morrison, and Mt Milligan, and elsewhere. Other circular/ring-like DT signatures are also defined across the Berg survey area, including at Bergette, whereas Tara/Sibola lies along strike with a linear conductive feature in the TPR and DT (Figure 4ab).

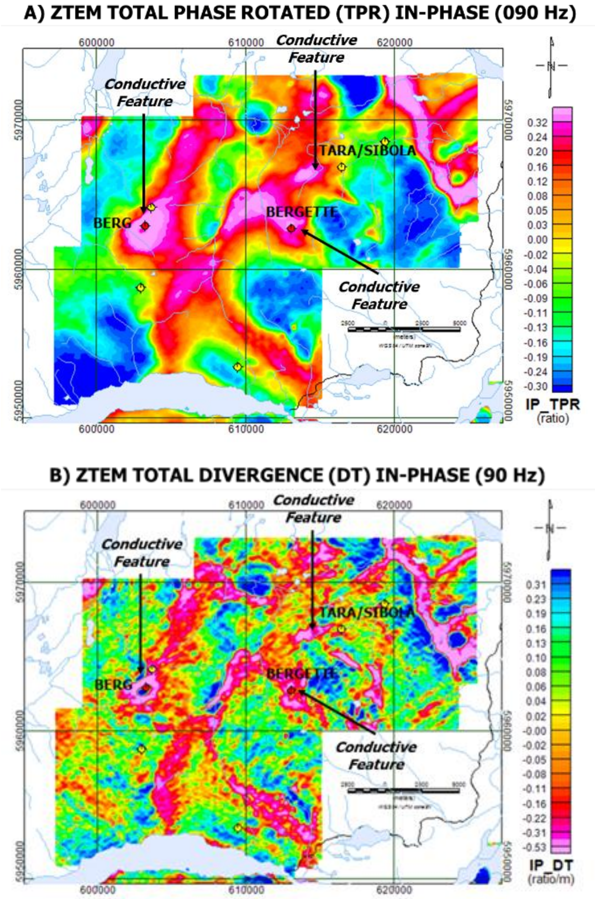

Figure 5: a) ZTEM In-phase Total Phase Rotation (TPR) at 90Hz, and b) Total Divergence (DT) at 90Hz, showing Berg porphyry and other occurrences from Figure 2, and highlighting some features of interest.

ZTEM and Magnetic Inversion Results

The ZTEM data have been converted to equivalent resistivity-depth distributions using 2D and 3D ZTEM inversions, with the Geotech Av2dtopo code (Legault et al., 2012) and UBC MT3dinv code (Holtham and Oldenburg, 2008), respectively. Both the 2D and 3D inversions account for topography and used 500 and 750 ohm-m half-space apriori start models, respectively. Figure 6a presents the 2D resistivity depth slice at -300m and Figure 6b presents the 3D inversion result at -300m depth. Both depth slices are shown with identical colour bars (~100-3k ohm-m). The images in Figure 5ab resemble each other reasonably well, including well defined conductive centre that coincides with the main Berg porphyry. However, the 3D inversion depth slice defines additional conductive anomalies not observed in 2D, particularly over Bergette.

Figure 6 presents the corresponding 3D magnetisation amplitude depth slice at -300m, obtained from the Geosoft VOXI MVI 3D inversion code (Ellis et al., 2012), which accounts for magnetic remanence. Berg is clearly marked by a ring-like magnetisation high that surrounds a low magnetic core, most likely reflecting alternating magnetite enrichment and depletion due to hydrothermal alteration. In contrast, as seen in the RTP results, Bergette and Tara/Sibola both coincide with high magnetisation amplitude signatures.

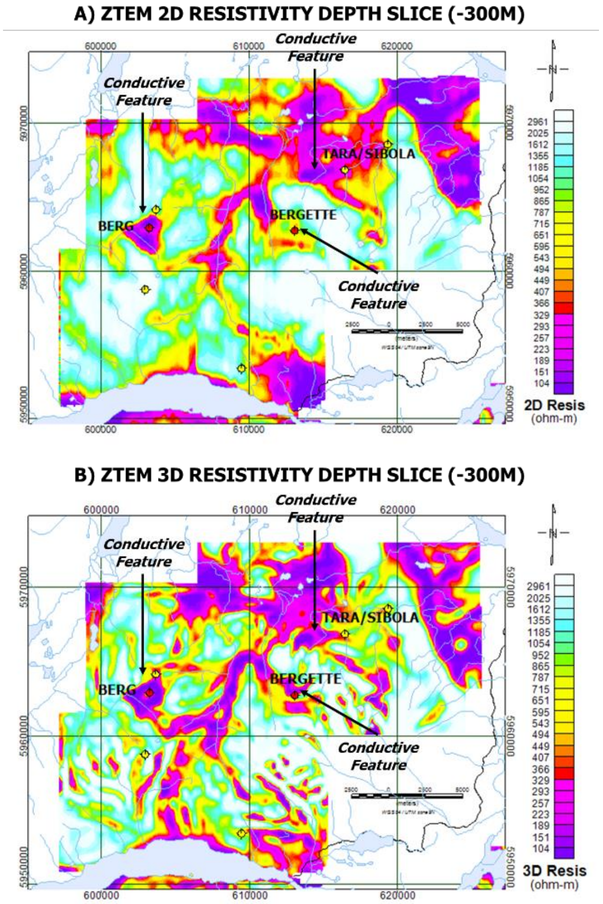

Figure 6: a) ZTEM 2D resistivity depth slice at -300m depth, and b) ZTEM 3D resistivity (red polygon) at -300m depth, highlighting some features of interest.

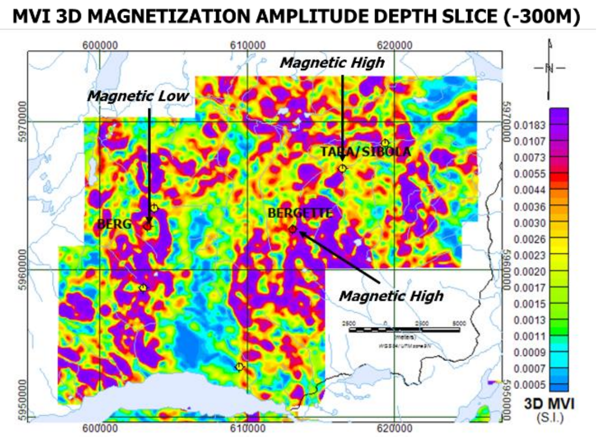

Figure 7: 3D MVI magnetisation amplitude depth slice at -300m depth, highlighting some features of interest.

Figure 8 presents the multi-parameter 2D and 3D inversion results as cross-sections along north-south line L1200 across the centre of the Berg porphyry copper deposit. Figures 7bc compare the ZTEM resistivity cross-sections obtained using 2D and 3D inversion. As shown, the ZTEM signatures from both inversions over Berg porphyry, which feature a slightly more resistive inner core that is surrounded by a more conductive outer shell, agree with the annular lithologic, mineralisation and alteration halo known to exist at Berg. The 3D inversion results further suggest that Berg's conductive phyllic halo extends to great depth as well as outward into the country rocks. Figure 7a presents the corresponding 3D MVI magnetisation amplitude section for L1200. The section shows that Berg occurs in a relative magnetic susceptibility low, likely reflecting magnetite depletion due to porphyry related hydrothermal alteration.

ZTEM 3D Synthetic Modeling

Results of 3D ZTEM synthetic modeling of the schematic Berg porphyry deposit are presented in Figure 9. The ZTEM modelling utilized an unstructured tetrahedral grid and a mimetic finite difference code based on the MT modelling program presented by Jahandari and Bihlo (2021). Figure 9c shows the calculated tipper response for 90 Hz. The ZTEM tipper values successfully indicate the presence of the porphyry deposit model, significantly overprinted by topographic effects.

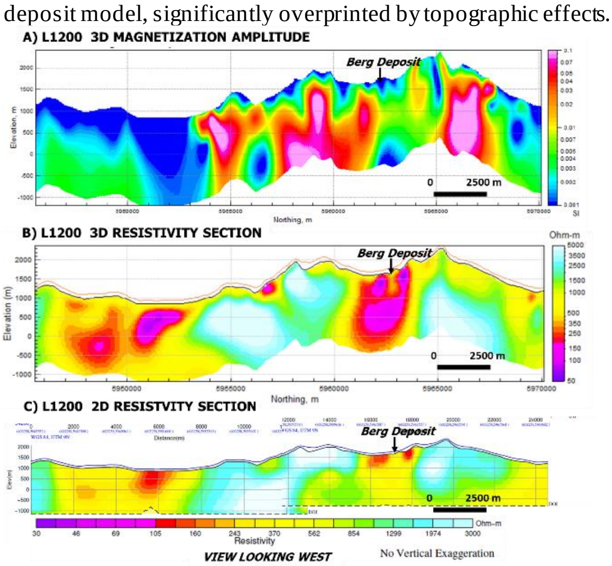

Figure 8: Multi-parameter 2D-3D inversion cross-sections along north-south L1200 across Berg porphyry deposit: a) 3D MVI magnetisation amplitude inversion; b) 3D ZTEM resistivity inversion, and c) 2D ZTEM resistivity inversion.

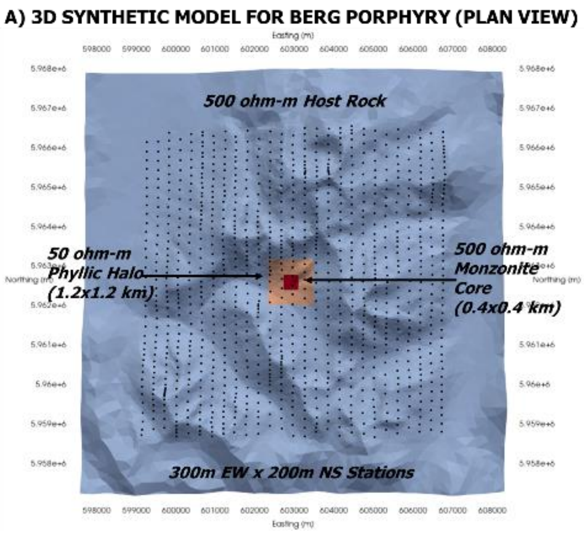

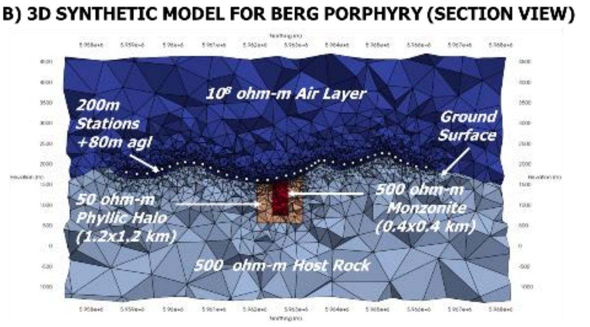

Figure 9: 3D ZTEM synthetic model for Berg porphyry deposit: a) Plan view of 3D model showing ZTEM tipper sites on topography approximated using tetrahedral grid mesh design; b) NS cross section view showing tetrahedral grid mesh design of subsurface resistivity model.

Mineral Targeting Porphyry Copper Deposits

Using recent examples of semi-automated, machine-learning assisted targeting using airborne geophysics applied to orogenic and epithermal gold-silver (Kwan and Legault, 2023; Legault et al., 2023), a similar mineral targeting approach has been tested for hidden porphyry copper deposits using the Berg ZTEM and magnetic survey results. The approach uses a semi-automated, machine-learning (ML) assisted method that includes: Structural Complexities (SC), Self-Organizing Map (SOM) classifications, and Supervised Deep Neural Network (SDNN) targeting of the geophysical data.

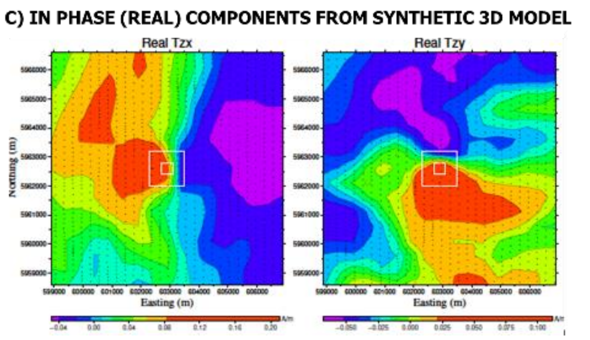

Figure 10: Calculated In-phase tippers for 3D ZTEM synthetic model of Berg porphyry deposit presented in Figure 9.

Self-Organizing Map (SOM) are useful tools in analysing and classifying multiple datasets. The magnetic SC data (COD + OE), the 3D ZTEM inversion data (-300m resistivity depth-slice), and the 3D MVI inversion data (-300m magnetisation amplitude depth-slice) were used as inputs and classified using the Geosoft SOM GX tool (https://geosoftgxdev.atlassian.net). As shown in Figure 11, the anomalous SOM classes (12 to 17) coincide with the known porphyry copper occurrences, namely Berg and Bergette, as well as lesser showings.

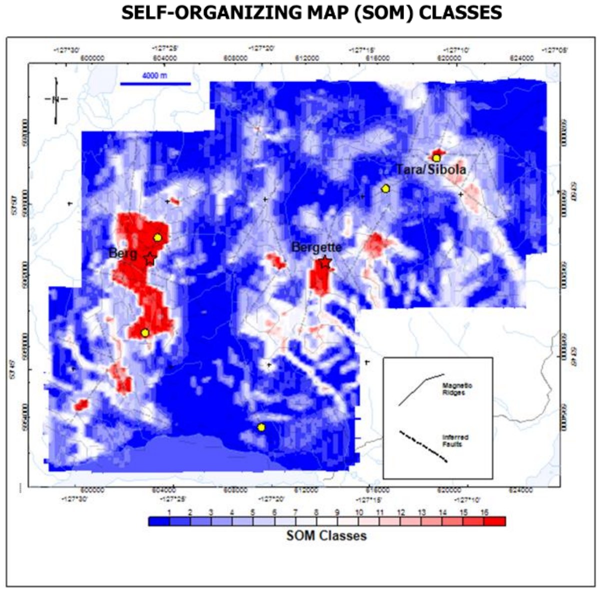

Figure 10: Self Organizing Map (SOM) results, showing anomalous SOM classes covering all the known porphyry copper occurrences, including Berg and Bergette.

The final mineral targeting step used the Supervised Deep Neural Network (SDNN) module in Google TensorFlow version TF 2.30 (https://www.tensorflow.org/). The training of the SDNN was performed on the Berg deposit area (Figure 12) using the magnetic COD and OE layers, the SOM classification results, the ZTEM 3D -300 m resistivity depth slice, and the MVI 3D -300 m magnetisation amplitude depth slice information,. The top 3.3% probability was selected for porphyry targeting (Figure 11b).

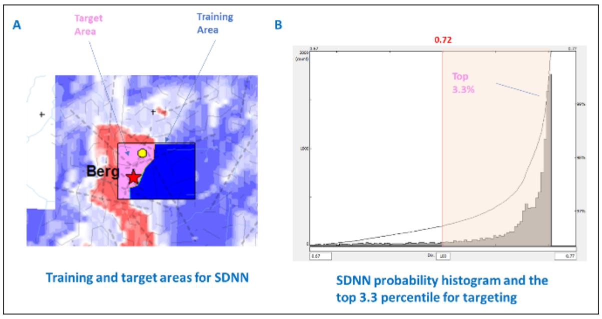

Figure 12: (A) Berg deposit training area for SDNN, (B) top 3.3% target probability cut-off for targeting.

The SDNN targeting was then applied to the entire Berg survey area, using similar multi-parameter data inputs as used in the initial SDNN training. Figure 12 presents the top 3.3% targeting probabilities over the DEM data, and the selected targets, T1-T4, which include Berg (T1) and Bergette (T2) as well as two other targets that also host known mineral showings and therefore represent potential areas for follow-up.

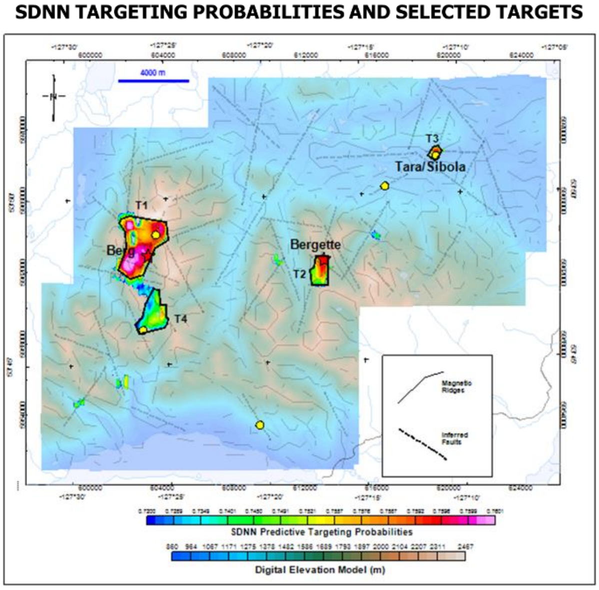

Figure 12: The SDNN top 3% probabilities over the DEM data and the selected potential porphyry targets (T1-T4), including Berg (T1) and Bergette (T2).

CONCLUSIONS

The ZTEM and magnetic results from the Berg Project present an excellent opportunity to study the geophysical signatures over an undeveloped yet significant porphyry copper deposit and the surrounding region. The Berg survey has led to the successful characterisation of the known porphyry deposit based on resistivity and magnetic susceptibility. The ZTEM survey results, assisted by 2D and 3D inversions, appears to map all the known porphyry deposits and occurrences at Berg, including the Bergette target. 2D-3D inversion analyses appear to confirm the bedrock source of conductivity that extend from surface to >500m depths. The magnetic and ZTEM results at Berg closely resemble those previously found in ZTEM surveys in the Western Cordillera, such as Morrison, Pebble, and Mt Milligan, including alteration-related, ring-like conductive highs that surround higher resistivities in the core and similar ring-like magnetic highs surrounding magnetic lows in the porphyry centres. The magnetic response is expected to be caused by magnetite enrichment in the outer halo and depletion in the centre. The increased conductivity within the mineralized porphyries at Berg show reasonable correlation with moderate to weak intensity phyllic alteration associated with hypogene mineralisation.

Finally, an approach for porphyry targeting has been tested, which uses a semi-automated, machine-learning (ML) assisted method that includes: Structural Complexities (SC), Self-Organizing Map (SOM) classifications, and Supervised Deep Neural Network (SDNN) targeting of the geophysical data. SC analysis of magnetic results has shown a close relationship between areas of structure intersection density and orientation diversity and the known porphyry occurrences. The SOM analysis showed the most anomalous classes coincide with the known porphyry copper occurrences, and other showings. Finally, the SDNN analysis, using Berg deposit as a training area, identified four main target areas that include both Berg and Bergette, as well as two other known mineral showings and that represent potential areas for follow-up.

ACKNOWLEDGMENTS

The authors wish to thank Surge Copper Corp. and Geotech for allowing us to present these results. We thank Hormoz Jahandari for contributing the 3D ZTEM synthetic modelling.

REFERENCES

Allard, M., 2007, On the Origin of the HTEM Species: In "Proceedings of Exploration 07: Fifth Decennial International Conference on Mineral Exploration" edited by B. Milkereit, 2007, p. 355-374.

Burge, C., 2014, A new porphyry copper deposit at Cobre Panama project: presented at PDAC Prospectors and Developers Convention, Discoveries and Developments session, Toronto, Canada.

Ellis, R.G., de Wet, B., and Macleod, I.N., 2012, Inversion of magnetic data for remanent and induced sources: 21ST ASEG Annual Conference and Exhibition, Extended Abstracts, 4 p.

Holden, E.-J., Wong, J. C., Kovesi, P., Wedge, D., Dentith, M., Bagas, L., 2012. Identifying structural complexity in aeromagnetic data: An image analysis approach to greenfields gold exploration. Ore Geology Reviews 46: 47–59.

Holtham, E., and Oldenburg, D.W., 2008, Three-dimensional forward modelling and inversion of Z-TEM data: 78TH SEG Annual International Meeting, Expanded Abstracts, 564-568.

Holtham, E., and Oldenburg, D.W., 2010, Three-dimensional inversion of ZTEM data: Geophysical Journal International, 182, 168-182.

Hoschke, T., 2011, Geophysical signatures of copper-gold porphyry and epithermal gold deposits, and implications for exploration: CODES-ARC Center of Excellence in Ore Deposits, University of Tasmania, 47 p.

Izarra, C., Legault, J.M. and Latrous, A., 2011, ZTEM airborne tipper AFMAG results over the Copaquire porphyry, northern Chile: 81ST SEG Annual International Meeting, Expanded Abstracts, 1257-1261.

Jahandari, H., and Bihlo, A., 2021, Forward modelling of geophysical electromagnetic data on unstructured grids using an adaptive mimetic finite-difference method: Computational Geosciences, 25, 1083-1104.

Kwan, K., and Legault, J.M., 2023, Gold targeting of fixed wing aeromagnetic Data using structural complexity, self-organizing map and supervised deep neural network analyses: A case study from the Red Lake camp, Superior Province, Ontario, Canada: Unpublished abstract submitted to IMAGE 2023 conference.

Labson, V. F., Becker, A., Morrison, H.F., and Conti, U. [1985] Geophysical exploration with audio frequency natural magnetic fields. Geophysics, 50, 656–664.

Lee, B.M., Unsworth, M., Hubert, J., Richards, J.P., and Legault, J.M., 2017, Geophysical Prospecting, 6, 397-421.

Legault, J.M., 2012, Ten years of passive airborne AFMAG EM development for mineral exploration: 82ND SEG Annual International Meeting, Expanded Abstracts, 5 p.

Legault, J.M., Wijns, C., Izarra, C., and Plastow, G., 2016, The Balboa ZTEM Cu-Mo-Au porphyry discovery at Cobre

Panama: 25TH ASEG-PESA-AIG Geophysical Conference and Exhibition, Extended Abstracts, 6 p.

Legault, J.M., Jahandari, H., and Ebert, S., 2022, ZTEM airborne natural field EM and magnetic case study over the Berg porphyry copper project, Huckleberry District, British Columbia: IMAGE, expanded abstracts, 5 p.

Legault, J.M., Kwan, K., Greig, J., Webster, E., and Hanki, M., 2023, Targeting epithermal Au-Ag using helicopter TDEM, magnetic, and radiometric data at Lawyers Project, North-Central BC, Canada: Unpublished expanded abstract submitted to AEM 2023 conference.

Lo, B., and Zang, M., 2008, Numerical modelling of Z-TEM (airborne AFMAG) responses to guide exploration strategies: 78th SEG Annual International Meeting, Expanded Abstracts, 1098-1101.

Norton, C., Huang, J., and Lui, D., 2021. Updated Technical Report and Mineral Resource Estimate on the Berg Project, British Columbia: Technical (NI 43-101) report to Surge Copper Corp., prepared Tetra Tech Canada Inc., 146 p.

Paré, P., Gribenko, A.V., Cox, L.H., Cuma, M., Wilson, G.A., Zhdanov, M.S, Legault, J.M., Smit, J. and Polomé, L., 2012, 3D inversion of SPECTREM and ZTEM airborne electromagnetic data from the Pebble Cu-Au-Mo porphyry deposit, Alaska: Exploration Geophysics, 43, 104-115.

Purich, E., Ray, B., Barry, J., Hayden, A., Yang, D., Schmidtt, H.R., 2016, Updated Resource Estimate and Preliminary Economic Assessment on the Ootsa Property, British Columbia, Canada: NI 43-101 Technical Report (No. 306) for Gold Reach Resources Ltd., by P & E Mining Consultants Inc. 433 p.

Sattel, D., Thomas, S. and Becken, M., 2010, An analysis of ZTEM data over the Mt Milligan porphyry copper deposit, British Columbia: 80th SEG Annual International Meeting, Expanded Abstracts, 1729–1733.

Sattel, D. and Witherly, K., 2012, Extracting information from ZTEM data with 2D inversions: 21ST ASEG Annual Conference and Exhibition, Extended Abstracts, 4 p.

Surge Copper Corp., 2021, Surge Copper Announces 2021 Exploration Plans: Press Release May 12, 2021, www.surgecopper.com.